

# Post-Earthquake Settlement of Levees on Peat

## Tassement post-sismique de digues sur sol organique

A. Lemnitzer

*University of California Irvine, Irvine, USA*

Riccardo Cappa

*Simpson, Gumperts & Heger Consulting Engineers, Irvine, USA*

Samuel Yniesta

*Ecole Polytechnique de Montréal, Montréal, Canada*

Jonathan Stewart, Scott Brandenberg

*University of California Los Angeles, Los Angeles, USA*

**ABSTRACT:** The seismic stability of embankment structures atop organic soils is controlled by the cyclic performance of the embankment fill and the response of the underlying foundation soil. Centrifuge testing at small (1m) and large (9m) scale was performed to study the seismic interaction between a model levee and the underlying peat. The levee-peat response was evaluated using extensive model instrumentation. Excess pore pressures developed in the peat during shaking were analyzed to compute secondary compression settlement rates due to cyclic straining. Post-seismic rate increases in secondary compression settlements of 18% and 52% were documented directly underneath the levee and in the free field arrays of the model, respectively. This suggests a strong potential hazard for accelerated long term crest settlements (i.e. reduction of freeboard) following seismic events, in particular for areas with minimal pre-earthquake secondary settlement rates. A newly developed nonlinear consolidation software package that follows an implicit finite difference formulation is introduced and experimental results are compared to numerical predictions. The software includes secondary compression deformation of soft soils concurrently with primary consolidation. Results indicate that secondary compression may control settlements in peat; therefore the influence of cyclic straining on secondary compression is an important consideration in design and retrofit of current/future embankment structures.

**RÉSUMÉ:** La stabilité sismique des structures de remblai sur les sols organiques est contrôlée par la performance cyclique du remblai et par la réponse du sol de fondation sous-jacent. Des essais en petite (1m) et grande (9 m) centrifugeuse ont été effectués pour étudier l'interaction sismique entre un modèle de digue et la tourbe sous-jacente. La réponse du système est mesurée en utilisant une instrumentation détaillée. Les pressions interstitielles en excès qui se développent dans la tourbe pendant les séismes ont été analysées pour calculer les taux de tassement de compression secondaire dus à la contrainte cyclique. Des augmentations du taux de tassement de compression secondaire post-sismique de 18% et 52% ont été enregistrées sous la digue et dans le champ libre du modèle, respectivement. Ceci suggère un fort risque d'accélération du tassement de la crête à long terme (c'est-à-dire la réduction de la revanche) suite à des événements sismiques, en particulier dans les zones avec des taux de tassement secondaires minimaux avant le séisme. Un nouveau logiciel de consolidation non linéaire est introduit et les résultats expérimentaux sont comparés aux prédictions numériques. Le logiciel

inclut la déformation de compression secondaire des sols meubles en même temps que la consolidation primaire. Les résultats indiquent que la compression secondaire peut contrôler les tassements dans la tourbe et que l'influence des déformations cycliques sur la compression secondaire peut contrôler la conception des digues..

**Keywords:** Levees; soil-structure interaction; secondary compression; settlement; embankment; peat

## 1 INTRODUCTION

Levees rest atop peat in many seismically active areas in the world. For example, Tsai et al. (2017) present a levee system in Hokkaido, Japan that was strongly shaken by earthquakes in 1993 and 2003. Preliminary results indicate that levees resting atop peat are more susceptible to earthquake-induced damage than levees resting on inorganic soils. The Sacramento-San Joaquin Delta in northern California has an extensive system of 1800 km of levees, many of which rest atop peat soil. The Delta serves as the hub of California's freshwater delivery system, and lies in an area with moderate seismic hazard (Figure 1). A well-understood driver of seismic deformation potential is liquefaction of saturated granular levee fill and/or foundation soils. By comparison, the seismic deformation potential of peat has received very little attention, but is potentially a significant hazard for levees.

Although peat is not susceptible to liquefaction, it is known to develop pore pressure during cyclic loading (e.g., Wehling et al. 2016). Furthermore, it is highly compressible and exhibits high secondary compression behavior (Mesri and Ajlouni 2007). Shafiee et al. (2015) found that cyclic loading can accelerate secondary compression behavior. Therefore, a significant concern is settlement following seismic loading and potential loss of freeboard of the levee structures.

Primary consolidation and secondary compression behavior are often assumed to occur at different times, with primary consolidation occurring prior to  $t_p$  and secondary

compression occurring after. This assumption results in a unique end-of-primary (EOP) normal consolidation line (NCL). Based on this "traditional" approach, secondary compression volume change is formulated as a function of time (Eq. 1), where  $C_a$  represents the coefficient of secondary compression,  $e_0$  is the initial void ratio,  $H_0$  is the thickness of the layer,  $t$  designates time and  $t_p$  is the time at the "end of primary consolidation".

$$S_s = \frac{C_a}{1+e_0} H_0 \log \frac{t}{t_p} \quad (1)$$

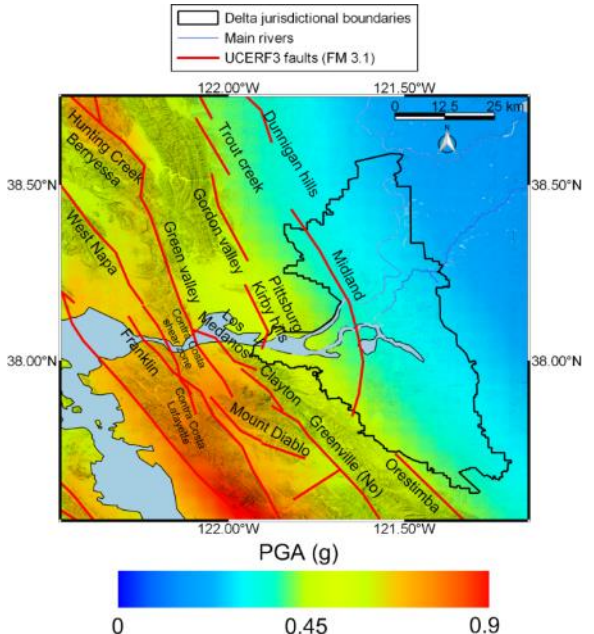


Figure 1. PGA Hazard Map for the Delta region (475yrs return period). (Deverel et al. 2016).

An alternative interpretation is that secondary compression occurs simultaneously with primary consolidation, resulting in an EOP NCL that depends on the consolidation time, and therefore on layer thickness. Bjerrum (1967) developed the time-line concept that is consistent with this idea.

In this study, a centrifuge test program consisting of non-liquefiable levees resting atop peat are performed to explore these different approaches to modeling primary consolidation and secondary compression. The experimental program is first described briefly, followed by settlement observations and predictions associated with various assumptions about secondary compression behavior.

## 2 EXPERIMENTAL STUDIES

To better understand the cyclic and post-cyclic performance behavior of levee structures on soft peat, and to gain an in-depth understanding of settlement rates in organic soil as function of excess pore pressure development during and after cyclic loading, an extensive series of centrifuge experiments were performed. These tests were conducted on the 1m and 9m radius geotechnical centrifuges located at the Center for Geotechnical Modeling at the University of California, Davis. The specific experiment selected for discussion consisted of a non-liquefiable levee made of modeling clay placed atop a layer of peat to study the settlement response of the organic foundation soil. Experiment reports, test data and media documentation of all investigations associated with the levee project are available through the DesignSafe cyberinfrastructure (Rathje et al., 2017) and the testing program is described in detail by Lemnitzer et al. 2015.

### 2.1. Large scale experiment on the 9m centrifuge

The prototype model constructed on the 9m radius centrifuge, hereafter labeled as Exp.14,

consists of a 5.1m thick levee overlying 6.1m of peat over 8.6m of dense coarse sand as shown in Figure 2. The model was instrumented with accelerometers, linear potentiometers, pore pressure transducers and bender elements to capture the static (slow data, e.g. consolidation process) and dynamic (fast data, e.g. ground motion) response of the system. The levee crest and base widths are 10.3 m and 30 m, respectively, and side slopes are 2:1. The levee was constructed from oil-based modeling clay with a unit weight around 16 kN/m<sup>3</sup>. The dense layer of coarse sand was placed via dry pluviation at the bottom of the container, and had a unit weight of 20.2 kN/m<sup>3</sup> and an approximate relative density  $D_R$  of 90%. The peat was recovered from a depth of 2-3 m at Sherman Island in the Delta and transported to the centrifuge facility. General peat properties obtained from laboratory testing are shown in Table 1. The virgin peat contained long fibers and clusters that were removed prior to placement in the centrifuge to obtain a more homogeneous material suitable for the centrifuge model (see Figure 2).

*Table 1: General properties of Delta peat*

| Property  | Measured      |
|---|---------------|
| Initial water content, w                                  | 670-870%      |
| Average organic content, OC                               | 69%           |
| Initial total unit weight, $\gamma_t$ , kN/m <sup>3</sup> | 10.28 – 10.41 |
| Specific Gravity of Solids, Gs                            | 1.79          |
| Initial Void Ratio, $e_0$                                 | 12 – 15.5     |
| Ave. Compression Index Odometer, Cc                       | 3.9           |
| Recompression Index Cr                                    | 0.4           |
| Secondary Compression Index Ca                            | 0.195         |

Following spin-up, each model was allowed to consolidate until excess pore pressures were essentially zero (approximately one hour) prior to applying a variety of ground motions. Dashed lines in Figure 3 indicate the initial position of the levee and peat prior to spinning. During spin up and primary consolidation at 57g, the peat in the center levee array settled approximately 4.16m in prototype scale - this settlement

corresponds to 40% vertical strain. The free field peat settled about 2.0 m in prototype scale, which corresponds to 21% vertical strain.



Figure 2. Coarse particles in sampling peat

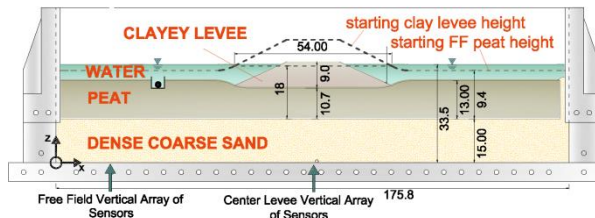


Figure 3. Setup of the 9m clay-levee experiment (Exp 14) following primary consolidation (all dimensions in prototype scale, instrumentation not shown).

## 2.2. Small scale experiment on the 1m centrifuge

Following the completion of the large scale experiments, additional testing on the 1m radius centrifuge was conducted to specifically study the effects of secondary compression and pore pressure development in an isolated, component-type investigation. This experiment is labeled Exp.16. A modeling clay levee of identical material as used for the 9m radius experiments was shaped to prototype dimensions of 2m in height, 10m in base width, 5m in crest width and slopes of 5:4.

The levee was placed on a layer of consolidated peat with a thickness of 3.5m in prototype scale. The bottom layer consisted of Nevada sand with a thickness of 1m. The peat and sand materials properties were identical to those used in the 9m radius experiments. Figure 4 depicts the setup of

the 1m radius centrifuge experiment prior to spinning.

The small scale model was first over-consolidated at 60g and then continuously spun at 50g. Ground motions were applied at the centrifugal acceleration of 50g. The model was instrumented with pore pressure transducers (P), linear potentiometers (LP) and accelerometers (A) as shown in Figure 3.

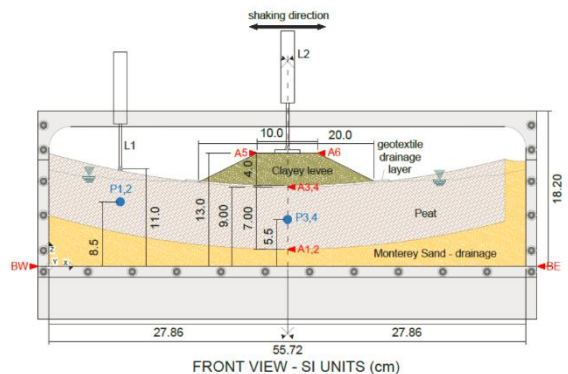


Figure 4. Setup of the 1m radius experiment @ 1g, prior to spinning (all dimensions in model scale, experiment labeled Exp 16).

## 2.3. Settlement Observations

Settlements were recorded using the external and internal instrumentation placed around the model (i.e., linear potentiometers, accelerometers). For the large scale 9m experiment, the Kobe ground motion with a prototype scale acceleration of 0.56g was selected for data analysis. This motion generated the largest pore pressure and settlement response in the peat.

The largest observed settlement was measured by sensor L11 mounted on the levee crest (Figure 5). Settlements in the free field were modest due to the difference in vertical effective overburden pressure (i.e., approx. 50 kPa below the center of the peat layer where the levee is located, compared with approx. 3 kPa in the free field).

A zoomed-in version of the model response during spinning is shown in Figure 5 before and

after the Kobe motion, which occurred at about time = 21,000 seconds in both figures. Figures 5 presents "slow data" sampled at 1Hz, which is too slow to capture the dynamic response of the model. "Fast data" sampled at over 4000 Hz is publicly available, but is not presented here for brevity. The Kobe motion generated excess pore pressures of about 6.93 kPa in the peat beneath the center of the levee. Approximately 25.6 cm of co-seismic settlement occurred, while an additional 22.9 cm occurred after shaking, before application of the next ground motion in the sequence. The settlement is divided among the following components: co-seismic settlements of approximately 6.3 cm, and post-seismic settlements (i.e., primary consolidation and secondary compression) of 19.3 cm were recorded. Following earthquake application, the model was allowed to enter the secondary compression stage before applying the next ground motion.

Figure 6 depicts the pore pressure development and settlements of the 1m centrifuge experiment at the center of the model (i.e., underneath the levee structure). The Maule motion generated an increase of pore pressures  $\Delta u$ , of 3.16kPa and a co-seismic settlement of 5.0cm. Settlements were recorded using LVDT L4, which was placed atop the levee structure, similarly to Exp. 14.

### 3 NUMERICAL SETTLEMENT STUDIES

Settlement predictions are performed using the iConsol.js finite difference nonlinear consolidation code (Brandenberg 2017). Secondary compression strain rate is formulated as a function of position in e-log  $\sigma'_v$  space relative to the NCL, enabling secondary compression to occur simultaneously with primary consolidation. The code is publicly available as a web-based application called "iConsol.js" at:

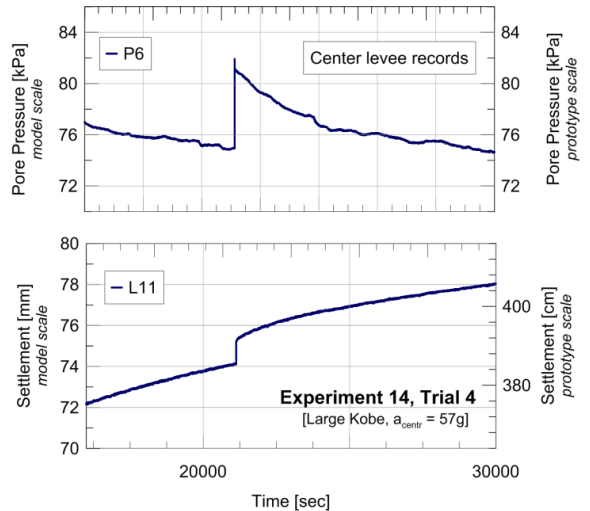


Figure 5: Co- and post seismic pore pressure and settlement records during the large Kobe motion in the center levee array for Exp 14 (9m Centrifuge)

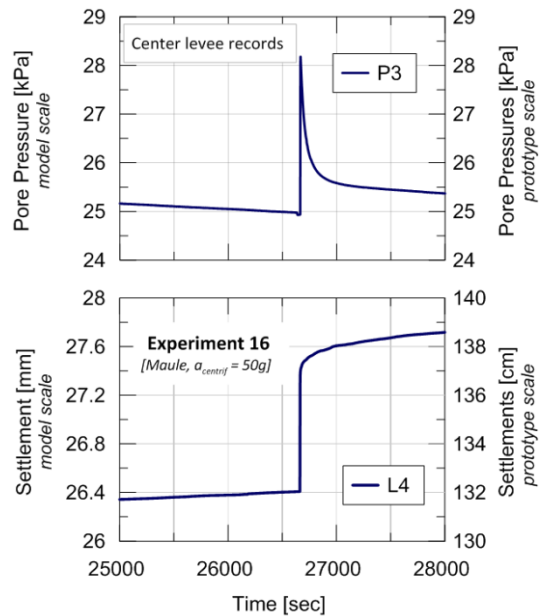


Figure 6: Co- and post seismic pore pressure and settlement records during the Maule motion in the center levee array for Exp 16 (1m radius Centrifuge)

[www.uclageo.com/Consolidation/](http://www.uclageo.com/Consolidation/). Residual excess pore pressure ratio,  $r_{u,r}$ , and secondary compression reset index,  $I_R$ , are computed based

on Shafiee (2016), as defined in Eqs. 2 and 3, where  $\gamma_c$  is equivalent cyclic strain amplitude,  $N$  is equivalent number of uniform cycles,  $OCR$  is overconsolidation ratio,  $OC$  is organic content,  $\alpha = \tau_s/\sigma_{vo}'$  is the static shear stress ratio,  $p_a$  is atmospheric pressure, and  $\gamma_{tp}$  is the threshold shear strain for pore pressure generation. Values of  $\gamma_c$  and  $N$  are computed from broadband strain histories using a procedure described by Cappa et al. (2017).

$$r_{u,r} = 0.316(\gamma_c - \gamma_{tp})^{0.619} \cdot N^{0.187} \cdot OCR^{-0.477} \cdot OC^{-0.499} \quad (2)$$

$$I_R = \gamma_c^{0.219} N^{0.261} (0.899\alpha + 0.939) \times (-0.043OC + 0.300) \left( 0.192 \frac{\sigma_{vo}'}{p_a} \right) \times (0.009OCR + 0.980) \quad (3)$$

The value of  $I_R$  ranges from 0 to 1, and represents reset of the secondary compression "clock". A value of  $I_R = 0$  involves no reset, while a value of  $I_R = 1$  returns the soil to its normally-consolidated secondary compression behavior. This is accomplished using the concept of a reference secondary compression line (RSCL), which is initially coincident with the NCL. The value of  $I_R$  marks the amount by which the RSCL is shifted from the NCL to the current state in e-log(sv') space.

To obtain an objective comparison between settlements measured in the centrifuge models and estimations using iConsol.js, the input parameters for compressibility, secondary compression, and permeability were selected from laboratory tests on peats reported by Shafiee (2016) and Cappa et al. 2017 (Table 1). Specifically, the normal consolidation line parameters were based on the e-log  $\sigma_v'$  relationships observed during consolidation testing in the laboratory. Permeability parameters were estimated from falling head tests. Secondary compression properties were

obtained from the consolidation test. By using the soil properties as reported by Shafiee who tested a wide range of peats to develop the regression formulations as described above, we are able to perform the settlement predictions as "blind predictions". Therefore input parameters reflect the peat tested by Shafiee (2016) and Shafiee et al. 2013 that is closest to our peat. We found this selection more meaningful, as a design engineers in "real-world" design scenarios would only have a limited amount of information available to conduct such analyses. The secondary compression reset was modeled using the "advanced" setting in the input window by reducing the value of  $e_{ca,ref}$  by an amount proportional to  $I_R$  multiplied by the difference in void ratio between the RSCL and the stress condition prior to imposing the Kobe motion. The overconsolidation ratio was computed based on the measured settlement at the time of application of the Kobe motion. Figure 7 shows a screen shot of the input parameters available in the iConsol software package.

Figure 8 (a&b) depicts a comparison of recorded and predicted settlements in the center levee array following the Large Kobe earthquake motion. Three different predictions were performed: (1) primary consolidation only (i.e., with  $C_a = 0$ ), (2) primary consolidation and secondary compression with no reset (i.e.,  $I_R = 0$ ), and (3) primary consolidation and secondary compression accounting for reset induced by the deviatoric strain history mobilized during the Kobe motion.

The analyses become progressively more accurate as  $C_a$  and  $I_R$  are introduced. The comparison shows clearly that secondary compression is the primary source of settlement, with primary consolidation contributing a relatively small fraction. Primary consolidation is small for this problem because the excess pore pressure ratio was only 0.086 (as calculated by Eq. 2).

|  |            |
|--|------------|
| <b>Compressibility Properties</b>                            |            |
| Virgin Compression Index, $C_c$                              | 3.9        |
| Recompression Index, $C_r$                                   | 0.4        |
| Reference Pressure, $\sigma'_{v,ref}$                        | 100 kPa    |
| Reference Void Ratio, $e_{\sigma',ref}$                      | 5.4        |
| Specific Gravity of Solids, $G_s$                            | 1.85       |
| <b>Permeability Properties</b>                               |            |
| Reference Permeability, $k_{ref}$                            | 2e-7 m/s   |
| Reference Void Ratio, $e_{k,ref}$                            | 6.3        |
| Coefficient of Permeability Variation, $C_k$                 | 1.5        |
| <b>Secondary Compression Properties</b>                      |            |
| Secondary Compression Input Type:                            | Advanced ▾ |
| Secondary Compression Index, $C_\alpha$                      | 0.195      |
| Reference Time, $t_{ref}$                                    | 86400 s    |
| Reference Void Ratio, $e_{c\alpha,ref}$                      | 4.678      |
| Reference Vertical Effective Stress, $\sigma'_{c\alpha,ref}$ | 100 kPa    |
| <b>Loading Conditions</b>                                    |            |
| Height, $H$  | 3.42 m     |
| Initial Overburden Pressure, $\sigma_0$                      | 47.7 kPa   |
| Vertical Total Stress Change, $\Delta q$                     | 0.0 kPa    |
| Initial Excess Pore Pressure Ratio, $r_u$                    | 0.086      |
| OCR  | 1.243      |
| Number of Elements, N  | 100        |
| Number of Time Steps   | 100        |
| Max Time, $t_{max}$  | 5.444e5 s  |
| Convergence Tolerance, tol                                   | 1.0e-8     |
| Drainage Boundary Condition                                  | Double ▾   |

Figure 7. Sample input screen in iConsol for the settlement analysis of the 9m radius experiment under the Kobe ground motion.

Furthermore, settlement is under-predicted when secondary compression reset is ignored. Only a correct inclusion of the reset mechanism (i.e. the integration of the accelerated secondary compression rate after seismic loading) is able to capture the measured settlements and yield an accurate prediction of the results. While both analysis options without the compression reset substantially underpredict the experimental settlements, accounting for the reset approximates the experimentally recorded values within an accuracy of 15%. Finally, the amount of settlement at the end of primary consolidation (around 2000 seconds for Fig. 8a, and 260 seconds for Fig. 8b, model scale) is smaller than the measurements and the predictions that include secondary compression. This is a clear indication that secondary compression occurs simultaneously with

primary consolidation, which supports the time-line concept adopted in the iConsol.js code. The rate of settlement measured in the centrifuge models may differ from the rate predicted by the iConsol.js code because the centrifuge models were two-dimensional, whereas the simulations are one-dimensional. This may partially explain why the settlement rate is faster in the experiments compared with the predictions.

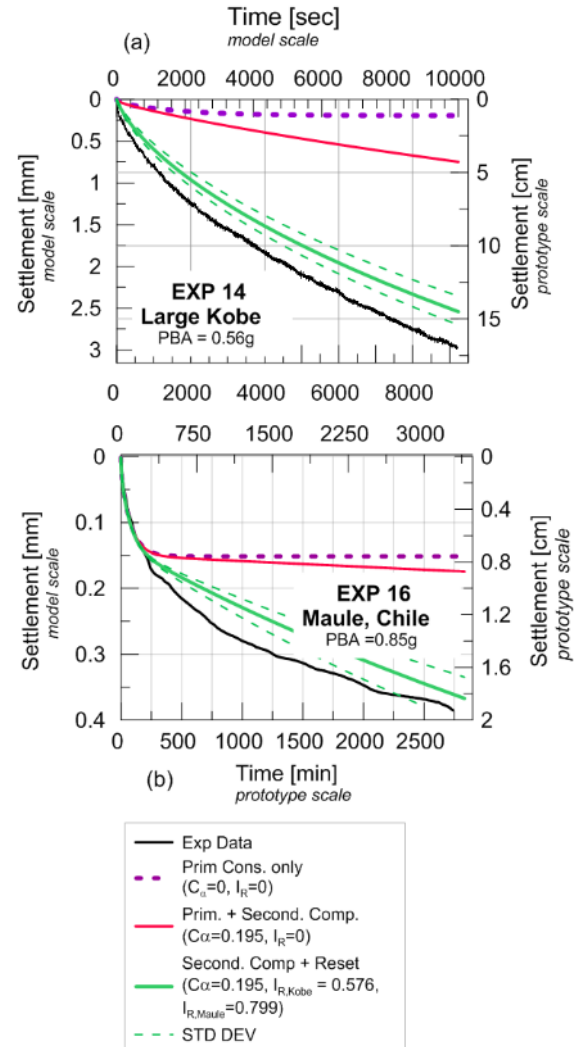


Figure 8. Settlement comparison between measure post cyclic record with predictions using the iConsol software by Brandenberg (2017)

## 4 CONCLUSIONS

Post-cyclic settlement of non-liquefiable levees resting atop peat soil observed in centrifuge models were predicted well by one-dimensional numerical models representing secondary compression and reset of secondary compression due to cyclic loading. Analyses that ignore secondary compression and its reset significantly under-predicted the observed settlements. Furthermore, simulations that ignore secondary compression under-predict observed settlements at the time of the end of primary consolidation. This is an indication that the two mechanisms occur simultaneously, and under-predictions may arise from the "traditional" method for computing secondary compression settlement.

## 5 ACKNOWLEDGEMENTS

This research was funded by the National Science Foundation under grant No. CMMI 1208170. The writers would like to acknowledge the valuable assistance of the UC Davis centrifuge team.

## 6 REFERENCES

- Bjerrum, L. 1967. "Engineering geology of Norwegian normally consolidated marine clays as related to settlements of buildings." *Geotechnique*, 17(2), 83–118.
- Brandenberg, S.J. 2017. iConsol.js: JavaScript Implicit Finite-Difference Code for Nonlinear Consolidation and Secondary Compression. *International Journal of mechanics*, ASCE [http://dx.doi.org/10.1061/\(ASCE\)GM.1943-5622.0000843](http://dx.doi.org/10.1061/(ASCE)GM.1943-5622.0000843)
- Cappa, R., Brandenberg, S.J. and Lemnitzer, A. 2017. Strains and pore pressures generated during cyclic loading of embankments on organic soil. *Journal of Geotechnical and Geoenviromental Engineering*, ASCE 143 (9).
- Deverel, A.J., Bachand, S., Brandenberg S.J., Jones C.E., Stewart, J.P., Zimmaro, P. (2016)."Factors and processes affecting Delta levee system vulnerability". *San Francisco Estuary and Watershed Science*, 14(4), Article 3
- Llemnitzer, A., Cappa, R., Yniesta, S. and Brandenberg, S.J. (2015) "Centrifuge Testing of Model Levees atop Peaty Soil: Experimental Data", *Earthquake Spectra*, <http://dx.doi.org/10.1193/032715EQS048>
- Mesri, G. and Ajlouni, M.A. 2007. Engineering Properties of Fibrous Peat, *Journal of Geotechnical and Geoenvironmental Engineering*, 133(7): 850-866.
- Rathje, E.M., Dawson, C., Padgett, J.E., Pinelli, J.-P., Stanzione, D., Adair, A., Arduino, P., Brandenberg, S.J., Cockeril, T., Esteva, M., Haan, F.L. Jr., Hanlon, M., Kareem, A., Lowes, L., Mock, S., and Mosqueda, G.. (2017). "DesignSafe: A new cyberinfrastructure for natural hazards engineering." *Natural Hazards Review*. 18(3).
- Shafiee, A. 2016. Cyclic and post-cyclic behavior of Sherman Island Peat, *PhD Dissertation*, University of California, Los Angeles.
- Shafiee, A., Stewart, J.P., and Brandenberg, S.J. 2015. Reset of secondary compression clock for peat by cyclic straining, *Journal of Geotechnical and Geoenvironmental Engineering*, ASCE, 141(3).
- Tsai, Y.T., Brandenberg, S.J., Kayen, R.E., Mikami, A. (2017). "Dataset for Empirical Assessment of Seismic Performance for Levees Founded on Peaty Organic Soils" GeoRisk Conference, Denver, Colorado | June 4-7, 2017
- Wehling, T.M., R.W. Boulanger, R. Arulnathan, L.F. Harder and M.W. Driller 2003. Nonlinear dynamic properties of a fibrous organic soil, *Journal of Geotechnical and Geoenvironmental Engineering*, ASCE, 129(10): 929-939.